International Journal of Image and Graphics

OPTIMAL RATE ALLOCATION FOR LOGO WATERMARKING

YUANWEI LAO
Department of Electrical and Computer Engineering
The Ohio State University
Columbus, Ohio 43210, USA
laoy@ece.osu.edu

YUAN F. ZHENG*
Department of Electrical and Computer Engineering
The Ohio State University
Columbus, Ohio 43210, USA
zheng@ece.osu.edu

Received (Day Month Year)
Revised (Day Month Year)
Accepted (Day Month Year)

Compression of logo as an image is addressed in logo watermarking, in which a framework of joint Human Vision System (HVS) model and rate allocation theory in the wavelet domain is applied. Under this framework, a novel logo watermarking algorithm using reversible discrete wavelet transform is proposed. Based on multi-level wavelet decomposition of both host and logo images, a well-known HVS model is applied to locate the visually insensitive area in the host for embedding, while the rate allocation theory determines how the logo is compressed and embedded by using the statistical characteristics of the logo. For a given overall embedding distortion, quantization step-sizes of different logo subbands are analytically determined to maximize the fidelity of the extracted logo under the imperceptibility constraint. The adaptive system is thus applicable to different hosts and logos without tuning the parameters manually. It is proved to be robust against various types of attacks and is quite suitable for hardware implementations. Since logo is considered as an image in this new algorithm, the watermarking approach developed can be extended in general to image-in-image embedding.

Keywords: Watermark; logo; Reversible Wavelet Transform (RWT); Human Vision System (HVS); rate allocation.

1. Introduction

When duplication and transmission of multimedia contents are getting ever easier in this information era, how to protect the content from unauthorized uses has become

*Corresponding author

an urgent task for the owners of the intellectual properties. *Digital watermarking* has become one of the most promising technologies and thus drawn much attention in recent years.[1,2,3] A watermark, normally either a sequence of bits or a meaningful logo, is securely inserted into the host before distribution and, if necessary, extracted to identify the ownership of the content.

Two major application scenarios, data authentication and copyright protection, require different properties of watermarking. Algorithms for the former are named fragile watermarking, in which the watermark should be easily corrupted to detect any intentional alteration. For the latter, watermarking should be imperceptible, robust, and secure. Imperceptibility means that the watermarked multimedia is visually identical to the original, while robustness assures that the embedded data survives both unintentional manipulations and malicious processing. In terms of security, only the original distributor or the authorized parties are able to extract the watermark even if the embedding method is legitimately published, which is usually achieved by using cryptographic keys. Intuitively, the more the watermark information is embedded, the more distortion it causes to the host. Therefore the key to a good watermarking algorithm is to minimize the required volume of data for embedding while achieving a reasonable level of robustness.

1.1. *Related Work*

There have been two perspectives to approach the watermarking problem, theoretical and practical. In the first category, a major problem is to find the fundamental limit, such as the capacity of watermarking in the host, in which multimedia data are abstracted into certain statistical distributions. Watermarking is then modeled as a communication channel with the host data considered as the side information, in which watermark is the message to be transmitted, and the embedder is playing an adverse game against the attacker. Cox et al. formally addressed this resemblance and classified the algorithms into three sub-categories according to the way of the side information used.[4] Silvestre et al.[5] and Mullarkey et al.[6] proposed various detection schemes to increase the robustness under the side-informed watermarking framework. Moulin and Ivanovic formulated watermarking as a min-max game over probability of error.[7] Cohen and Lapidoth calculated the coding capacities in different situations assuming Gaussian distributions for the host and attack involved.[8] Moulin and Mihcak further characterized watermarking and attacking as two banks of parallel channels, in which optimal distortion allocation was formulated by information theory, while the interaction between the embedder and the attacker was considered by the game theory.[9]

From the practical perspective, many watermarking algorithms using a variety of signal processing techniques have been proposed. The purpose is to reach the theoretical limit of watermarking in terms of imperceptibility, robustness and security. Of all the techniques, Discrete Wavelet Transform (DWT) based schemes have gained great popularity due to its high robustness against general attacks.[10]

In early days, Zhu et al. introduced a wavelet domain algorithm by performing multi-level decomposition to the host image and embedding all the watermark data into the high-pass subbands.[11] Dugad et al. presented a similar algorithm, while the embedding locations were selected by comparing the magnitude of DWT coefficients at each location with a fixed threshold.[12] Podilchuk et al. proposed another wavelet domain algorithm by using the just noticeable difference (JND) which employed a more flexible threshold for selecting embedding locations.[13] However, neither fixed threshold nor JND fully exploits the spatial features of the host image, which reveals most suitable locations for embedding in terms of imperceptibility of human eyes. The introduction of numerous Human Vision System (HVS) models has been proved effective for improving the robustness of watermarking. Based on Watson's observations[14] of noise visibility in different resolutions of the host image and Xia et al.'s multi-resolution techniques[15], Kim and Moon proposed an algorithm which used adaptive thresholds,[16] while Hien et al. introduced an algorithm suitable for multi-information embedding by using redundant wavelet transform and independent component analysis based on the calculation of the same noise visibility function.[17] Barni et al. borrowed the idea of perceptual weights from Lewis [19] and applied it successfully to sequence watermarking.[18] Meanwhile, some researchers have attempted to improve the performance by taking advantage of the inherent tree structure [20] of multi-resolution subbands using DWT to embed the watermark accordingly,[21,22,23,24] while others have tried to integrate watermarking into the image compression process.[25,26]

As a subcategory of generic watermarking, *logo watermarking*, in contrast to conventional sequence watermarking, is visually more meaningful and thus has more practical applications. One major advantage is that the adaptive filtering ability of human perception could help recognize the extracted logo instantaneously, which is not possible by using sequence watermark detection. A number of researchers have made significant contributions to this field. Hsu and Wu explored the pyramid structure of a binary logo and embedded it into the different subbands of DWT-decomposed host image.[27] Niu et al. converted the gray-scale logo into bit-planes and inserted them into different DWT decomposed subbands.[28] Kundur and Hatzinakos performed a milestone work for logo watermarking, which embedded one-level DWT decomposed logo into multi-level decomposed host image based on an HVS model by calculating a perceptual index, called "Salience".[29] By integrating the idea of perceptual weights,[19] Reddy and Chatterji extended Barni et al.'s results[18] to logo watermarking.[30] Xie and Shen, on the other hand, focused on the extraction end and designed a blind logo extraction method, in which discrete cosine transform (DCT) was performed on the logo.[31,32] First and Qi also combined the conventional additive approach with a modulus one in the approximate subband for blind logo watermarking.[33]

Blind algorithms, as opposite to non-blind ones, are more convenient due to the fact that the original host image is not required for logo extraction. However, the main concern of copyright protection is robustness, and non-blind algorithms

are considered more capable to achieve higher robustness than blind ones. Besides, in many applications, the host image is available if the original owner wants to firmly verify the copyright. Therefore, how to improve robustness under a non-blind watermarking framework will be the focus of this work.

1.2. *Outline of Our Approach*

Compared to a bit sequence, a logo is represented by a much larger volume of data and contains lots of redundancy. In all the previous works, reducing this redundancy was not a primary concern. It has been considered that for logo watermarking, the logo image has to be optimally compressed to minimize its impact to the quality of the host image, and the compression mechanism should not cause too much distortion for feasible recognition of the extracted logo, which unfortunately affects the quality of the host in an adverse way since a less distorted logo needs more data and vice versa. As a result, there is a tradeoff between the distortion of the host and that of the logo. Unfortunately, how to optimize this tradeoff in logo watermarking has never been theoretically studied before. In any optimization process, one should define the goal of optimization under a set of given constraints. For the current tradeoff problem, the goal is to minimize the distortion to the extracted logo while that to the host is constrained by a predefined level. This is a reasonable goal-constrained setting because the fidelity of the host image can only be sacrificed by a limited amount in trading for the protection; otherwise, logo watermarking will defeat the original purpose.

In this paper, a new logo watermarking algorithm is presented to optimize the tradeoff as just described. Rather than a general DWT used for decomposition,[29] the algorithm makes use of the reversible wavelet transform (RWT),[35] a transformative DWT, to decompose both host and logo images into multiple levels. The utilization of RWT is to facilitate the implementation of the algorithm in an embedded system due to the efficiency of integer-to-integer computation involved in RWT. After RWT, the coefficients of each logo subband are inserted into the corresponding subband of the host. In the embedding process, a well-known HVS model is utilized to automatically identify the most imperceptible areas of the host while formulating the distortion of the host. By using the statistical distribution of the coefficients of each logo subband, defined as the *logo side information*, the algorithm allocates energy to each subband of logo optimally by minimizing the distortion of the extracted logo subject to the constraint imposed on the distortion of the host. By doing all the above, a new logo embedding algorithm is obtained to maximize the robustness for copyright protection. It can guarantee the distortion level of the host while the distortion to the logo is minimized.

From the theoretical point of view, our work could also be considered as a form of spread spectrum (SS) watermarking in general because of spreading watermark coefficients over the frequency domain of the host image.[2] The focus and uniqueness of this work is to study how the logo coefficients could be optimally compressed

and distributed over the host to maximize the fidelity of the extracted logo, given the overall host distortion, compared to the close works,[18,29] where the property of the logo as an image has been generally ignored. It can also be regarded as a form of side-informed approaches summarized by Cox et al.[4] Rather than exploiting the host side information to optimize the detector design, both host and logo side information is used to achieve joint redundancy reduction and logo embedding in an optimal way. The optimality of the proposed scheme is not universal, but under the rate-allocation framework. The new algorithm is tested to be robust to various types of attacks. Our prior work on the subject was published as a conference paper.[34] Compared to that, this work has a more detailed and articulated presentation and includes more comparisons with other methods in terms of the fidelity of the extracted logos for different combinations of host and logo images. Besides, the extension of the new watermarking approach to the application of image-in-image embedding is considered in the current paper.

The rest of this paper is organized as follows. In Section 2, the new logo watermarking scheme is introduced. Theoretical derivation is presented in detail in Section 3. Numerical results are given in Section 4 to verify its improved performance over existing methods. Additional experimental results are provided to show the applicability of the new approach to general image-in-image embedding. Section 5 concludes this paper.

2. The Proposed Logo Watermarking Scheme

In this section, a novel logo watermarking scheme using multi-level reversible wavelet decomposition to both host and logo images is presented. L is used to denote the wavelet transform level of the host and h_i^b, x_j^b to denote the wavelet coefficients of the host and logo, respectively, where b is the subband index and i, j are the coefficient indices.

The central idea of the embedding mechanism is shown in Fig. 1, in which the suggested decomposition level is $L = 4$, and the logo is decomposed into $L - 1 = 3$ levels. The low-low frequency band (LL) of the host is not used for hiding since a small distortion in the LL subband could cause a relatively large artifact in the watermarked image. Instead, the logo LL subband is embedded into the high-high subband (HH) of the highest level of the host, as indicated by the top arrow in Fig. 1. For the remaining subbands, the logo coefficients are inserted into the corresponding host subbands with the same decomposition level and orientation. In other words, the logo subband b is associated with the host subband b for $b = 0, 1, \ldots, (3L - 2)$. The detail of the logo embedding scheme will be described after a review of RWT and the HVS model in the following.

2.1. *Reversible Wavelet Transform*

Reversible wavelet transform (RWT) has been widely used for lossless compression, especially in JPEG2000,[35] which involves only integer-to-integer computation.[36]

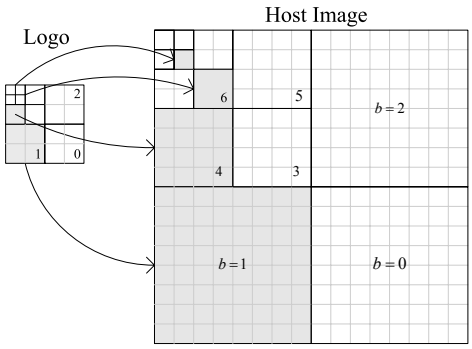

Fig. 1. The embedding diagram shows the level of decomposition and the embedding scheme.

Strictly speaking, RWT is not a conventional wavelet transform, but an approximation by performing non-linear truncation operations, which round the outputs to nearest integers. As opposite to the floating point arithmetic in generic DWT, RWT achieves high efficiency in its memory usage, which is the key feature for the convenience of hardware implementation. Besides, it enables a unified codec for both lossy and lossless compression. Popular reversible wavelet transforms are S, TS, S+P, 5/3, and the integer-version of bi-orthogonal (9,7), etc.[36] Since the ultimate objective of this work is to implement the algorithm into an embedded system for real-time applications, RWT is suitable purely due to its advantage of integer-to-integer computation and is selected in this paper. Note that regular DWT can be applied in this framework of watermarking as well. That is, the result of this work can be used to optimize rate allocation for watermarking with any family of wavelets. Performance difference, if any, is beyond the scope of this work and will not be addressed here.

2.2. *Human Vision System in the Wavelet Domain*

To guarantee imperceptibility, logo coefficients have to be hidden into the visually insensitive areas of the host image. Therefore a good HVS model, which defines the insensitive area, is of great importance for this purpose. The contrast sensitivity function (CSF) is one of the most popular measures used in DCT based image compression,[35] but it is not applicable for the wavelet domain. For the latter, Lewis first introduced a multi-resolution model for image compression,[19] while Barni et al. made some effective modifications to this comprehensive model and applied it to sequence watermarking, which took a number of factors into consideration, including luminance, orientation, and texture.[18] The latter model is adopted in our scheme. That is, a perceptual weight q_i^b is calculated for each host coefficient at

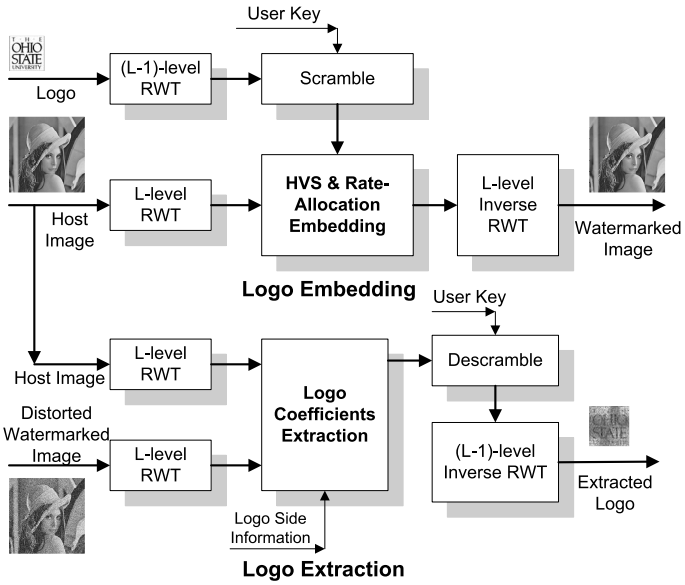

Fig. 2. The block diagram of the logo watermarking system.

location i in subband b except the LL subband, as given in the following equation

$$q_i^b = \frac{1}{2} \cdot \Theta(b) \cdot \Lambda(b,i) \cdot \Xi(b,i)^{0.2} \tag{1}$$

where $\Theta(b)$ associates a weight with each subband to indicate the sensitivity to noise changes due to its orientation and decomposition level.[18] $\Lambda(b,i)$ measures the brightness of that pixel and assigns high priority to the area which is either very bright or very dark, while $\Xi(b,i)$ measures the texture activity of the neighborhood by performing a linear weighted summation of mean square value of the wavelet coefficients in the current and higher level subbands. Overall Eq. (1) calculates how sensitive to noise a particular location is in the wavelet domain, which tells how much information is appropriate for embedding there.

2.3. *Logo Embedding*

The logo embedding system is shown in Fig. 2, and the detailed embedding procedure is described below.

Step 1. RWT and Scrambling: Perform L-level and $(L-1)$-level RWT on the host and logo images respectively to obtain the wavelet coefficients of each. The logo coefficients within each subband are then permuted for a given user key to generate the pseudo-random-like coefficients.

Step 2. Embedding in Significant Locations: The coefficients of each logo subband are embedded into the corresponding subband of the host as shown in Fig.

1. The perceptual weights q_i^b are calculated for the coefficients of a given subband b of the host by Eq. (1), and are then sorted in a descending order. Only the top P percentage of the most significant coefficients are selected for embedding and are denoted as h_i^b (the value of P will be discussed again in the next section). By using the logo side information which is the variances σ_b^2 of logo subbands, the quantization step-sizes Δ_b are analytically derived in Section 3 for all the subbands of the logo image. The coefficients of the watermarked host $\hat{h}_i^b$ are thus given by the following equation

$$\hat{h}_i^b = h_i^b + \lfloor (q_i^b \cdot x_j^b)/\Delta_b \rfloor, \tag{2}$$

where h_i^b is the coefficient of the host before the embedding, x_j^b denotes the coefficient of the logo, and $\lfloor \cdot \rfloor$ is the truncation operation due to RWT. Note that the number of h_i^b could be significantly larger than that of x_j^b. As a result, each logo coefficient could be embedded multiple times. By using the above equation, the logo image is compressed because the coefficients of the logo are represented by fewer bits following the quantization which reduces the impact to the host. One may notice that in Eq. (2), the perceptual weight q_i^b is also involved, which is to adjust the logo coefficient according to the imperceptibility of the host coefficients.

Step 3. Inverse RWT: Perform the inverse RWT to the modified coefficients of the host, which generates the watermarked image.

2.4. *Logo Extraction*

The lower part of Fig. 2 shows how the logo is extracted, which is reverse to the process of logo embedding and involves two tasks. One is to recover the logo coefficients, and the other is to estimate and compensate the potential distortion to the logo. An effective compensation method is to perform a linear weighted combination of the recovered copies of the coefficients, by which the quality of the extracted logo can be improved.[29,30] However, the main focus of this work is to show how optimal rate allocation could improve the overall performance as opposite to considering the host image only. So the rest of the new scheme is made simple by averaging multiple copies of the extracted coefficients to facilitate the theoretical derivation in Section 3 although the weighted method can still be integrated into our scheme with a higher computational cost. Using the averaging method, the procedure of logo extraction of our new scheme is described formally below.

Step 1. RWT: Perform L-level RWT on both the original host and watermarked images.

Step 2. Recovery: The same perceptual weights in the embedding procedure are calculated based on the original host to find the embedding locations. As far as the logo is concerned, only the logo side information is required in this step to obtain the quantization step-sizes Δ_b as mentioned earlier. Thus the logo coefficients are recovered by the following equation

$$\tilde{x}_j^b = (\hat{h'}_i^b - h_i^b) \cdot \Delta_b / q_i^b, \tag{3}$$

where $\hat{h'}_i^b$ is the potentially distorted coefficient of the watermarked image. Since the coefficients of the logo are embedded multiple times, all the corresponding copies of each coefficient are simply averaged to obtain the final value:

$$\hat{x}_j^b = \lfloor (\sum_k \tilde{x}_k^b)/N_j^b \rfloor, \tag{4}$$

where N_j^b is the number of the embedding times for that coefficient and is counted during the extraction process.

Step 3. De-Scramble and IRWT: The extracted coefficients $\hat{x}_j^b$ of the logo are de-scrambled, and the inverse RWT is applied to the coefficients to generate the logo image.

Step 4. Optional Post-Processing: In this work, applications of 8-bit gray-scale images are considered. After RWT, embedding, possible attacks, and IRWT, the pixel values of the extracted logo may not fall into the range of $0 \sim 255$ or only occupy a subset. In order to enhance the visual quality of the logo and to render the best display effect on the terminal, an optional brightness adjustment could be performed on the extracted logo to obtain the final image, which linearly scales its pixel values to the range $0 \sim 255$ according to its minimum and maximum values.

In the extraction procedure, no original image for the logo is needed, but only the logo side information is required for a better detection. Since this information is also available at the owner end for non-blind watermarking algorithms, it will not sacrifice any usability. Besides, the volume of this side information is trivial compared to the logo image, and it could be easily stored in the system once the embedding is finished.

3. Optimal Rate Allocation

As mentioned in Section 1, the necessity for compressing the logo was not explicitly mentioned in the previous works of logo watermarking. Most of them adopted a global *scaling factor* to adjust the energy of the embedding logo implicitly. In this work, the logo is compressed by quantizing the coefficients, where the step-size of quantization is determined individually for each logo subband by a joint HVS analysis of the host and the statistical distribution of the logo coefficients in that subband. The current problem has its root in the generic framework of image compression using wavelet transform, such as JPEG2000.[35] The difference is that in generic image compression the interest is the optimal rate allocation for each subband which minimizes the distortion to the decompressed image given the overall coding rate, while in the current problem the interest is the optimal quantization step-sizes for subbands which minimize the distortion to the extracted logo given a permissible level of distortion to the host.

The pursuit of the current optimization problem is fundamentally reasonable because transmitting a quality host image is the ultimate goal of the owner that should be guaranteed even when seeking for the best copyright protection. The most

desirable solution would bring no distortion at all which is unfortunately not possible. Consequently, it can only compromise the quality of the host by an acceptable amount to exchange for the best protection of the copyright. The latter is equivalent to least distortion to the extracted logo. Given the goal and constraint, the current optimization problem can be mathematically formulated, and the solution can be found as discussed below.

3.1. *Problem Formulization*

As mentioned in the procedure of logo embedding in Section 2.3, the number of host coefficients used for embedding is not fixed, but defined by a percentage P, i.e., only the top P percentage of most significant host coefficients (according to the perceptual weights) in each subband are selected. A larger host image might have more significant coefficients. Assume each logo coefficient has been embedded for K_b times on average for subband b, and K_b is associated with P by the following,

$$W_b^L H_b^L \cdot K_b = W_b^H H_b^H \cdot P, \tag{5}$$

where W_b^L and H_b^L are width and height of the logo subband b, and similarly W_b^H and H_b^H are those of the host. Due to the innate property of the proposed scheme, the embedding number of logo LL subband, K_9 (when $L = 4$), is only a quarter of K_b for the rest subbands ($b = 0, ..., 8$), as shown in Fig. 1. For simplicity, limit K_b to integer. As a result, for a 512×512 host and a 64×64 logo, $W_9^L H_9^L = 2^6$, $W_0^L H_0^L = 2^{10}$ and $W_9^H H_9^H = 2^{10}$, $W_0^H H_0^H = 2^{16}$, and then $K_9 = 2^4 \cdot P$, $K_0 = 2^6 \cdot P$, i.e., when $P = \frac{1}{16}, \frac{1}{4}$, $K_9 = 1, 4$ and $K_0 = 4, 16$, respectively.

Let $d_H(\Delta_b)$ be the mean embedding distortion to the host and $d_L(\Delta_b)$ the mean distortion for each coefficient of the extracted logo, both of which will be defined in detail later. The current optimization problem is formulated as:

$$\begin{aligned} Minimize: \ & D_L(\Delta) = \sum_{b=0}^{B-1} \eta_b^L S_b^L d_L(\Delta_b) \\ Subject\ to: \ & D_H(\Delta) = P \sum_{b=0}^{B-1} \eta_b^H S_b^H d_H(\Delta_b) \leq \Omega \end{aligned} \tag{6}$$

where Ω is the limitation capping the mean embedding distortion to the host, $B = (3L - 2)$ is the number of the logo subbands, and η_b is the ratio of the number of coefficients in band b to the total number of coefficients. S_b is the synthesis gain of the wavelet filter (associated with the inverse wavelet transform) for band b, and $S_b = 1$ if the wavelet filters are ortho-normal. Since RWT filters are generally not ortho-normal, S_b varies for each subband depending on the choice of RWT. The superscripts L and H represent logo and host, respectively. The object function categorizes the overall distortion of the extracted logo due to the compression which is to be minimized, while the inequality denotes the constraint imposed on the overall embedding distortion of the host. Let us now move on to find the solution of the defined optimization problem.

3.2. *A Simplified Case*

Two steps are suggested to solve the optimization problem in Eq. (6). In the first step, the percentage P of the embeddable coefficients are assumed to be small, which simplifies the problem, while in the second step a more general solution is presented. The first step however is necessary en route for obtaining the final solution which will be made clear as our discussion proceeds.

When the embedding percentage P is relatively small, there are only few non-zero perceptual weights q_i^b in the host image. It is reasonable to assume that they are constant q^b within each subband. Thus Δ_b/q^b can simply be replaced by Δ_b, and Eq. (2) is reduced to

$$\hat{h}_i^b = h_i^b + \lfloor x_j^b/\Delta_b \rfloor. \tag{7}$$

Similar to JPEG2000,[35] the relationship between the distortion to the image and the quantization step can be expressed as $d_L(\Delta_b) = c\Delta_b^2$, where $c = 1/12$. On the other hand, the mean embedding distortion of the host is defined as the mean square of the integer part of a quantized logo coefficient, i.e., $d_H(\Delta_b) = E\{\lfloor x/\Delta_b \rfloor^2\}$. Let $x/\Delta_b = u + r$, where $u = \lfloor x/\Delta_b \rfloor$ and $r = \{x/\Delta_b\}$ are the integer and decimal parts of the quantized coefficient, respectively, and r has a uniform distribution on $[0, 1)$. It follows that

$$d_H(\Delta_b) = E\{u^2\} = E\{(\frac{x}{\Delta_b} - r)^2\} = E\{(\frac{x}{\Delta_b})^2\} - 2E\{\frac{x}{\Delta_b}r\} + E\{r^2\} = \frac{\sigma_b^2}{\Delta_b^2} + \alpha,$$

where α is a constant. $d_H(\Delta_b) = \sigma_b^2/\Delta_b^2$ is simply used in the following calculation since α can be absorbed into the constraint of Ω by moving the corresponding item to the right. Substituting $d_L(\Delta_b)$ and $d_H(\Delta_b)$ into Eq. (6) and using the Lagrange multiplier method,

$$L(\Delta_b, \lambda) = \sum_{b=0}^{B-1} \eta_b^L S_b^L c\Delta_b^2 + \lambda \left(P \sum_{b=0}^{B-1} \eta_b^H S_b^H \sigma_b^2/\Delta_b^2 - \Omega \right). \tag{8}$$

Taking the partial derivative of Eq. (8) with respect to each Δ_b, $b = 0, \ldots, (B-1)$ and λ, it becomes

$$\frac{\partial L(\Delta_b, \lambda)}{\partial \Delta_b} = 2\eta_b^L S_b^L c\Delta_b - 2\lambda P \eta_b^H S_b^H \frac{\sigma_b^2}{\Delta_b^3} = 0, \tag{9}$$

$$\frac{\partial L(\Delta_b, \lambda)}{\partial \lambda} = P \sum_{b=0}^{B-1} \eta_b^H S_b^H \sigma_b^2/\Delta_b^2 - \Omega = 0. \tag{10}$$

Combining these equations, the step-sizes are solved,

$$\Delta_b = \sqrt[4]{\lambda \sigma_b^2 \frac{\eta_b^H S_b^H}{c\eta_b^L S_b^L}}, \quad b = 0, 1, ..., (B-1), \tag{11}$$

where $\lambda = \left[P \cdot \left(\sum_{b=0}^{B-1} \sigma_b \sqrt{c\eta_b^H \eta_b^L S_b^H S_b^L} \right) / \Omega \right]^2$. One may notice that in this simplified case, HVS is only used for selecting the coefficients within each subband for

embedding, but not involved in determining the quantization step-sizes. A more general case is discussed next in which HVS is involved in both.

3.3. *Subband Grouping for Further Optimization*

If P is large, it is inappropriate to assume the perceptual weights to be constant within a subband. It is important to exploit the spatial variation within each subband of the host as well as that of the logo for variable quantization step-sizes. The idea of subband grouping was introduced and theoretically verified in JPEG 2000, which divides each subband of the wavelet coefficients into groups and determines the step-size for each group accordingly even within the same subband. In this way, a gain of up to $1.43\,dB$ can be achieved for the decompressed image.[35]

This idea is extended to the problem of watermarking. That is, both the perceptual weights of the host and the coefficients of the logo are divided into groups. By doing so, variations between groups could be exploited to hide more watermark energy. Similar to JPEG 2000, the coefficients of each logo subband are divided into Nc groups, and the perceptual weights of the top P percentage are thus divided into $K_b \cdot N_c$ groups. For simplicity, N_c is limited to be dyadic, such as $1, 4, 16$, etc. Hence in the embedding Eq. (2), the perceptual weight of each group has to be re-written as $q^b_{k,n}$, $k = 0, ., (K_b - 1); n = 0, ., (N_c - 1)$, and the step-size become $\Delta_{b,n}$. Thus each logo coefficient is recovered by averaging multiple copies of the quantized coefficients as

$$\hat{x}^b_{n,j} = \frac{1}{K_b} \sum_{k=0}^{K_b-1} \lfloor \frac{q^b_{k,n} \cdot x^b_{n,j}}{\Delta_{b,n}} \rfloor \cdot \frac{\Delta_{b,n}}{q^b_{k,n}}. \tag{12}$$

Then the corresponding distortion to the host and that to the logo are given as

$$D_H(\Delta) = \frac{P}{N_c} \sum_{b=0}^{B-1} \sum_{n=0}^{N_c-1} \eta^H_b S^H_b A_{b,n} \sigma^2_{b,n} / \Delta^2_{b,n}, \tag{13}$$

$$D_L(\Delta) = \frac{1}{N_c} \sum_{b=0}^{B-1} \sum_{n=0}^{N_c-1} \eta^L_b S^L_b B_{b,n} c \Delta^2_{b,n} \tag{14}$$

where $A_{b,n} = \frac{1}{K_b} \sum_k \left(q^b_{n,k}\right)^2$ and $B_{b,n} = \frac{1}{K_b} \sum_k 1/\left(q^b_{n,k}\right)^2$. Dividing logo coefficients into groups is equivalent to having more subbands. Thus the optimization problem could be solved by the same technique as the one used in the simplified case. Hence for each group, the optimal quantization step-sizes are

$$\Delta_{b,n} = \sqrt[4]{\lambda \frac{A_{b,n} \eta^H_b S^H_b}{c B_{b,n} \eta^L_b S^L_b} \sigma^2_{b,n}}, \quad b = 0, 1, ..., (B-1), n = 0, 1, ..., (N_c - 1), \tag{15}$$

where $\lambda = \left[\frac{P \cdot \sum_{i=0}^{B-1} \sum_{j=0}^{N_c-1} \sigma_{i,j} \sqrt{c A_{i,j} B_{i,j} \eta^H_i \eta^L_i S^H_i S^L_i}}{\Omega N_c} \right]^2$. The above discussion finally justifies why a two-step approach is necessary to find the solution of the general optimization problem.

(a) Lenna (b) Peppers

(c) Logo One (d) Logo Two (e) Logo Three

Fig. 3. The 512×512 host images and the 64×64 OSU logos.

Treating logo watermarking as a distortion minimization problem given the limitation of distortion to the host is the major contribution of this paper. The solution to the problem generates a new watermarking scheme which is especially suitable for embedding meaningful logo images. Since the latter usually contains a large amount of data, only when the embedding is optimized, distortion to both host and logo images can be practically minimized. This statement will be proved true through experiments as presented in the next section.

4. Experimental Results

In this section, a set of experiments is presented to verify the performance of the new scheme, which involves four steps. First the imperceptibility of the embedding method by subjective observations is evaluated. The gain of further grouping within the subband is demonstrated, and the relationship between the distortion of the host and that of the extracted logo is displayed to guide a good tradeoff. Secondly, the robustness of the scheme is tested against various kinds of attacks on different combinations of host images and logos. Thirdly, the proposed scheme is compared with an existing method, under the same RWT framework, to demonstrate its superiority and improved performance. Finally, experiments of general image-in-image embedding are performed to illustrate a wider scope of applications of the new embedding approach.

Table 1. Experimental Parameters

Wavelet Level (L)	4
No. of Groups (N_c)	4
Wavelet Type (RWT)	5/3 filter
Embed Percentage (P)	25 %

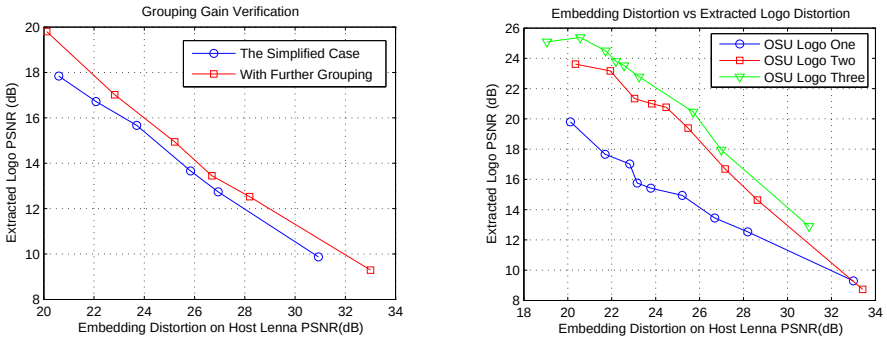

(a) Grouping gain verification with host Lenna. (b) Embedding distortion vs extracted logo distortion with host Lenna.

Fig. 4. Determine the imperceptibility

For all these purposes, two popular gray-scale host images, the 512×512 Lenna and the 512×512 Peppers, and three different 8-bit 64×64 OSU logos, are selected, as shown in Fig. 3. Though these logos are all in gray-scale, they differ significantly in content. Logo One is more like a black-and-white text logo, while Logo Three is purely a figure. Logo Two is a combination of text and figure. Different types of logos are expected to bring different watermarking effects, as shown in the following experiments. Since 5/3 filter is selected as the RWT, the corresponding synthesis gains are $S_b = 1, 1, 1, 2, 2, 2, 4, 4, 4, 8$ for $b = 0, 1, .., 9$, respectively. Related parameters are summarized in Table 1. The decomposition level L and the number of groups N_c are carefully selected according to the sizes of the host and logo images, and the wavelet type is one of the optional wavelets available in the system. The embedding percentage P is empirically determined through experiments, by which the average embedding time K_b can obtained by Eq. (5).

4.1. *Determine the Imperceptibility*

The first question is how much logo energy should be embedded into the host to obtain a good tradeoff between the imperceptibility of the host and the fidelity of the extracted logo. The more the logo energy is embedded, the more the distortion

it causes to the watermarked image and the higher the fidelity of the extracted logo could be. Therefore what the acceptable distortion to the host is should be determined first, i.e., the constraint of the proposed optimization problem.

Two series of watermarking processes with different embedding energy are performed with the host Lenna, and the curves of the distortions of the extracted logo against those of the watermarked image are drawn. In the first series, let us compare the performance between the simplified (circle) and the grouping (square) approaches on Logo One. The results are shown in Fig. 4(a), which clearly demonstrates that the grouping approach is better at all levels of the embedding energy. Then watermarking using the grouping approach is performed, and the three OSU logos are embedded individually to the host Lenna in the second series, as shown in Fig. 4(b). As expected, the performance varies for different logos, and Logo Three achieves a higher extraction fidelity than the other two given the same embedding distortion. By subjective observations of the three series, it shows that when the PSNR of the watermarked host is $21\,dB$ or higher as shown in Fig. 5(a), the embedding is imperceptible, and the watermarked Lenna (with OSU Logo One) is visually identical to the original in Fig. 3(a). Although the constraint could also be selected as high as $30\,dB$ or even higher, $21\,dB$ is selected as the constraint of optimization in all the following experiments in order to achieve the limit of robustness.

It is also worth noting that the difference image between the watermarked and the original host is plotted in Fig. 5(b), from which one can see where the logo energy is embedded. Notice that the visually insensitive areas, such as the highly textured hair and edges rather than plain areas, are used for embedding due to the combination of the HVS model Eq. (1) and the optimal rate allocation scheme. Without any attacks, the extracted logos are shown in the first columns of Fig. 6 and Fig. 7, respectively, which are almost identical to the original logos, but not exactly because of the quantization used during the embedding.

4.2. *Robustness Verification*

To test the robustness of the scheme, experiments on both host images are performed. First, three OSU logos are embedded into the host Lenna individually, resulting in embedding distortion PSNRs of 22.82, 23.04 and $21.72\,dB$, respectively, which are all higher than the constraint of $21\,dB$. The extracted logos without attacks are shown in the first column of Fig. 6, whose PSNRs are 17.02, 21.34 and $24.5\,dB$, respectively. Then various types of attacks, including additive Gaussian noise, average & median filtering, JPEG & JPEG2000 compression, are applied to the watermarked Lenna. The corresponding results are shown for each logo in Fig. 6, in which the PSNR indicates the fidelity of the extracted logo, while the parameter in the parentheses is the distortion degrading to the host due to each specific attack. Instead of displaying results under mild distortions, the attack parameters are pushed to the limit such that the extracted logos are just recognizable.

First, the watermarked Lennas are corrupted by additive Gaussian noise with

(a) Watermarked image with Logo One under the constraint of 21 dB (Actual PSNR=22.82 dB)

(b) Difference image (magnified by 8)

Fig. 5. Subjective evaluations on imperceptibility.

(a) Logo One: 17.02dB (No Attack); 7.948dB (D=11.13dB); 8.54dB (D=15.48dB); 9.245dB (D=16.94dB); 8.824dB ($QF = 20$); 8.869dB ($CR \approx 34$).

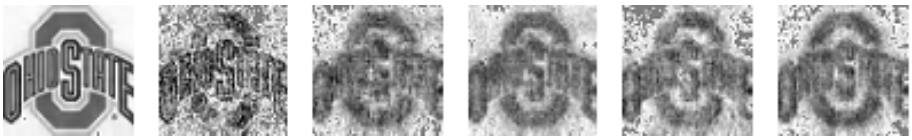

(b) Logo Two: 21.34dB (No Attack); 8.058dB (D=11.13dB); 7.78dB (D=15.51dB); 9.023dB (D=16.92dB); 8.36dB ($QF = 20$); 8.861dB ($CR \approx 34$).

(c) Logo Three: 21.72dB (No Attack); 11.25dB (D=11.1dB); 11.74dB (D=15.1dB); 12.88dB (D=16.94dB); 11.75dB ($QF = 20$); 11.64dB ($CR \approx 34$).

Fig. 6. Robustness verification I: host Lenna. (From left to right: no attack; noisy; 3×3 average filtering; 3×3 median filtering; JPEG; JPEG2000.)

a variance of 0.005, leading to a severe quality degradation of about $D \approx 11\,dB$ to the host. However, the extracted OSU logos are still visually recognizable, as shown

in the second column of Fig. 6. Then after 3×3 average or median filtering, the watermarked images are degraded by $15 \sim 16\,dB$. The extracted logos are given in the third and fourth columns of Fig. 6, respectively, which are still identifiable, although severely distorted. Next, the watermarked Lennas are compressed by JPEG with high compression ratios (CR) (or low quality factors). Quality factor (QF), ranging from 1 to 100, is a frequently used index in evaluating JPEG compression. The higher the QF is, the lower the CR is. When reducing QF down to 20 ($CR \approx 24$), the extracted logos are still recognizable in the fifth column of Fig. 6. Based on the same principle, the scheme is tested under the JPEG2000 compression. Amazingly, when CR is increased up to 34, the extracted logos in the sixth column are still as identifiable as the counterparts of JPEG with $CR \approx 24$, which shows that the proposed algorithm is very resilient against wavelet domain manipulations.

With the same settings, experiments are repeated with the host Peppers. As shown in Fig. 7, a similar performance as for Lenna has been achieved. After displaying the results under different attacks, it is also interesting to compare the extracting qualities between the three logos listed by rows in Figs. 6 and 7. Even though the embedding distortion of Logo Three, Fig. 6(c), is slightly stronger, the extracted logos are much more perceptible than the other two. For example, the QF of JPEG compression could be pushed even lower ($< 20dB$) for Logo Three, while $QF = 20$ almost reaches the lower bound of the recognizability of Logo One. The relatively simple pattern in Logo Three may account for this advantage.

4.3. *Performance Comparison*

Our new scheme is compared with an existing method. As mentioned before, the methods closest to the proposed one are reported in the previous works, which also use DWT to decompose and to embed the coefficients of the logo into the host subbands.[29,30] The embedding strategy of Reddy et al.[30] is selected for comparison since it has already achieved higher robustness than the other.

To obtain a meaningful comparison, host Lenna and Logo One are used with the same scaling factors of the one-level method,[30] i.e., $0.4 : 1$ for the LL and other subbands. The method achieves an embedding PSNR of $22.76\,dB$, which is very close to that of the proposed scheme, PSNR $= 22.82\,dB$ in Fig. 5(a). The extracted logo is as perceptible as ours as shown in Fig. 8(a). The same signal attacks to the watermarked images are applied. In the case of additive Gaussian noise, the extracted logo is given in the second column of Fig. 8(a), which is less identifiable than ours in Fig. 6(a). The extracted logos after both 3×3 average and median filtering are hardly recognizable and thus not shown here. Under the JPEG compression, the results for the QF as high as 50 are barely recognizable, as shown in the third column of Fig. 8(a), while it is still quite recognizable even for $QF = 20$ by the proposed new scheme as shown in Fig. 6(a). After JPEG2000 compression, using the existing method[30] with $CR \approx 17$, the result is shown in the fourth column, which is comparable with that of the proposed scheme as shown in

(a) Logo One: 17.13dB (No Attack); 7.866dB (D=12.96dB); 8.748dB (D=16.94dB); 9.321dB (D=18.4dB); 8.879dB ($QF = 20$); 8.811dB ($CR \approx 34$).

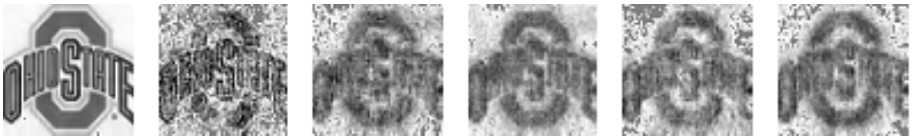

(b) Logo Two: 21.49dB (No Attack); 8.167dB (D=13.02dB); 8.13dB (D=16.88dB); 9.129dB (D=18.38dB); 7.569dB ($QF = 20$); 8.9dB ($CR \approx 34$).

(c) Logo Three: 24.89dB (No Attack); 10.07dB (D=12.95dB); 12.13dB (D=16.92dB); 13.91dB (D=18.4dB); 11.55dB ($QF = 20$); 11.79dB ($CR \approx 34$).

Fig. 7. Robustness verification II: host Peppers. (From left to right: no attack; noisy; 3×3 average filtering; 3×3 median filtering; JPEG; JPEG2000.)

Fig. 6(a), but the compression ratio of ours is much higher ($CR \approx 34$). A similar comparison with Logo Two and Logo Three over the host Peppers is also conducted, the extracted logos without attack, under noise, JPEG and JPEG2000 distortions are shown in Fig. 8(b) and Fig. 8(c), respectively, which could be used to compare with the results in Fig. 7.

The experiments with host Lenna under different compression ratios are repeated, and the results are plotted in Fig. 9. Under the JPEG compression (solid lines), the proposed scheme (triangle) achieves a higher fidelity of the extracted logo than the method (circle).[30] In the JPEG2000 case (dashed lines), a similar conclusion can be drawn for high compression ratios. From the results of all these experiments, one can summarize that the proposed scheme improves the robustness of the existing method significantly by exploiting the statistical knowledge of the logo.

4.4. *Extend to General Image-in-image Embedding*

Since logo is considered as an image, our new watermarking scheme can be extended generally to image-in-image embedding. Additional experiments are conducted to show the potential of this new application. Two well-known images, 128×128

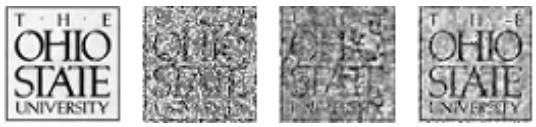

(a) Logo One (host Lenna): 19.46dB (No Attack); 7.53dB (AWGN D=11.08dB); 8.344dB (JPEG $QF = 50$); 9.0dB (JPEG2000 $CR \approx 17$).

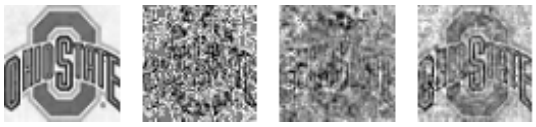

(b) Logo Two (Host Peppers): 18.61dB (No Attack); 6.988dB (AWGN D=12.99dB); 7.125dB (JPEG $QF = 50$); 9.346dB (JPEG2000 $CR \approx 17$).

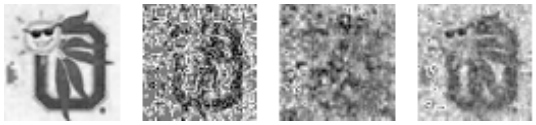

(c) Logo Three (Host Peppers): 19.97dB (No Attack); 7.541dB (AWGN D=12.98dB); 7.8295dB (JPEG $QF = 50$); 10.34dB (JPEG2000 $CR \approx 17$).

Fig. 8. Performance of an existing method. (From left to right: no attack; noisy; JPEG; JPEG2000.)

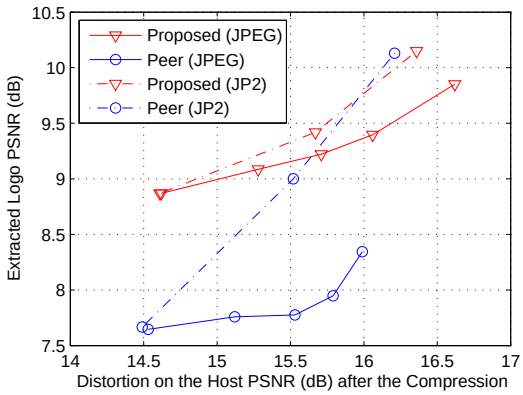

Fig. 9. Performance comparison under JPEG & JPEG2000.

Baboon and Jet, are chosen as shown in Fig. 10(a) and Fig. 10(d), respectively, to replace the relatively small logo. With the same procedure as in Fig. 2, Baboon or

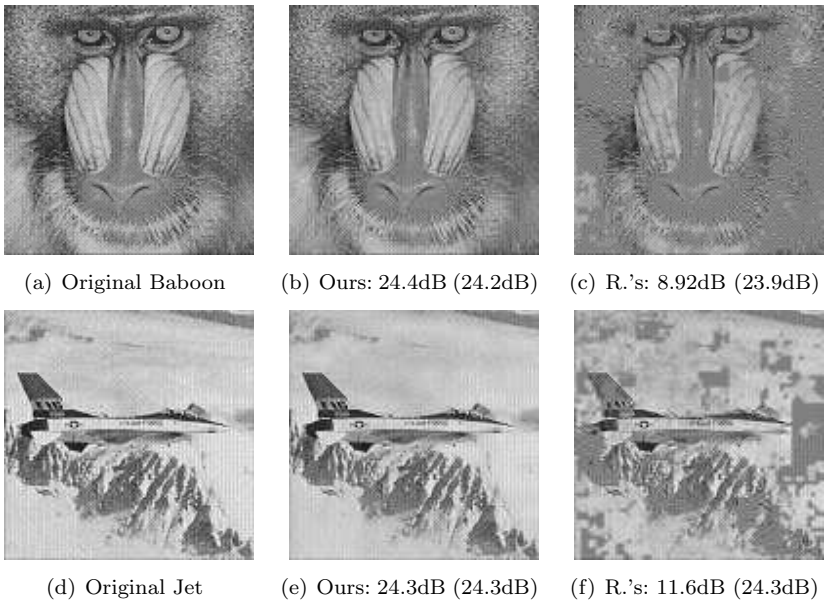

(a) Original Baboon (b) Ours: 24.4dB (24.2dB) (c) R.'s: 8.92dB (23.9dB)

(d) Original Jet (e) Ours: 24.3dB (24.3dB) (f) R.'s: 11.6dB (24.3dB)

Fig. 10. Extension to general image-in-image embedding (host Peppers).

Jet is 3-level decomposed, and the coefficients of each subband are inserted into the corresponding subband of the host Peppers.

Without any special parameter tuning, the extracted Baboon and Jet are shown in Fig. 10(b) and Fig. 10(e), respectively, where the PSNR is the distortion to the extracted image and the PSNR in the parenthesis denotes the embedding effect. By both subjective and quantitative evaluations, the proposed scheme works very well for these two relatively large images. The previous method[30] is used to perform the same image-in-image embedding. The results are shown in Fig. 10(c) and Fig. 10(f), respectively. As one can see for both images, the embedding distortion of the previous method is more severe, and the proposed scheme achieves a much higher extraction fidelity. The reason for such a big difference is because when the embedded image becomes large and complicated, the volume of the data representing it increases significantly. Only when the redundancy in the image is *optimally* reduced by a scheme like the one proposed in this paper, can image-in-image embedding produce a satisfactory result.

4.5. *Discussion*

The focus of this work is to improve the robustness of non-blind watermarking by taking the properties of the logo image into consideration, where optimal rate allocation is formulated to maximize the fidelity of the extracted logo, given the constraints on the distortion level of the host. The problem on how much distortion

to the host is acceptable (or the level of noise resiliency) is a fundamental issue relating to the human vision system, which still remains open and is beyond the scope of this paper. Since no model is claimed to truly represent the human vision system, the distortion of an image is still measured by PSNR in general, and only some empirical numbers of PSNR are considered acceptable, which varies for different images. For example, PSNR should be as high as $30\,dB$ on a generic image for human eyes to identify any noticeable distortion, while PSNR could be as low as $20\,dB$ for some highly textured images. In this work, the acceptable distortion is determined by subjective visual inspection of human eyes.

Another closely-related issue is the optimal number of host coefficients to embed a logo bit. Since the acceptable distortion level of an image remains uncertain, this optimal number is an unsolvable problem as well, which explains why empirical selection through experiments is used in this and some other works. It is only clear that this number should vary for different host images. For a relatively plain image, the number of host coefficients appropriate for embedding could be significantly less than that of a highly textured image.

5. Conclusions

Due to the importance of watermarking for copyright protection in general, and the merit of easy recognition of a meaningful logo in particular, logo watermarking continues to be an active topic of study in recent years. This paper has introduced a new logo watermarking scheme which features the joint compression and embedding of the logo to minimize the impact to the quality of the embedded host. By successfully exploiting the joint application of the HVS model and the rate allocation theory, a new RWT decomposition and compression algorithm is developed to achieve optimal energy allocation of the logo under the constraint of imperceptibility of the watermarked host. Logo embedding is thus formulated as an optimization problem for which solutions are found using the powerful Lagrange multiplier method. Once a single constrained threshold is selected, this adaptive algorithm could apply to different combinations of host and logo images.

Extensive experiments have verified that the new scheme is extremely powerful against various types of general attacks and has demonstrated a great potential in general image-in-image embedding. In comparison with a similar existing method, it has achieved improved performance in terms of robustness. By using RWT, this robust watermarking scheme is compatible with the JPEG2000 standard. That is, compression to the host and logo as well as watermarking can all be performed under the same framework of JPEG2000.

Acknowledgements

This work was supported by the National Science Foundation of USA under the grant IIS-0322802 and by its Chinese counterpart NFSC under grant 60632040.

References

1. I. J. Cox, M. L. Miller, and J. A. Bloom, *Digital Watermarking* (Morgan Kaufmann, San Francisco, CA, 2001).
2. I. J. Cox, I. Kilian, T. Leighton, and T. Shannon, "Secure spread spetrum watermarking for multimedia," *IEEE Trans. Image Processing* **6**(12), 1673 (1997).
3. F. A. P. Petitcolas, R. J. Anderson, and M. G. Kuhn, "Information hiding-a survey," in *Proc. IEEE* **87**, 1062 (1999).
4. I. J. Cox, M. L. Miller, and A. L. McKellips, "Watermarking as communications with side information," in *Proc. IEEE* **87**, 1127 (1999).
5. G. C. M. Silvestre, N. J. Hurley, and T. Furon, "Robustness and efficiency of non-linear side-informed watermarking," in *Revised Papers from the 5th International Workshop on Information Hiding*, (London, UK, 2003), p. 106.
6. M. Mullarkey, N. J. Hurley, G. C. M. Silvestre, and T. Furon, "Application of side-informed embedding and polynomial detection to audio watermarking," in *Proc. IEEE Int. Conf. Acoustics, Speech and Signal Processing (ICASSP)* **57** (2003).
7. P. Moulin and A. Ivanovic, "The watermark selection game," in *Proc. Conf. on Information Sciences and Systems*, (Baltimore, MD, 2001).
8. A. S. Cohen and A. Lapidoth, "The Gaussian watermarking game," *IEEE Trans. Information Theory* **48**(6), 1639 (2002).
9. P. Moulin and M. K. Mihcak, "The parallel-Gaussian watermarking game," *IEEE Trans. Information Theory* **50**(2), 272 (2004).
10. P. Meerwald and A. Uhl, "A survey Of wavelet-Domain watermarking algorithms," *Proceedings of SPIE, Electronic Imaging, Security and Watermarking of Multimedia Contents III*, (San Jose, USA, Jan. 2001).
11. W. Zhu, Z. Xiong, and Y.-Q. Zhang, "Multiresolution watermarking for images and video," *IEEE Trans. Circuits and Systems for Video Tech.* **9**(4), 545 (1999).
12. R. Dugad, K. Ratakonda, and N. Ahuja, "A new wavelet-based scheme for watermarking images," in *Proc. IEEE Int. Conf. Image Processing (ICIP)* (Chicago, IL, USA, Oct. 1998), p. 419.
13. C. I. Podilchuk and W. Zeng, "Image-adaptive watermarking using visual models," *IEEE J. Selected Areas in Communications* **16**(4), 525 (1998).
14. A. B. Watson, G. Y. Yang, J. A. Solomon and J. Villasenor, "Visibility of wavelet quantization noise," *IEEE Trans. Image Processing* **6**(8), 1164 (1997).
15. X. G. Xia, C. G. Boncelet, and G. R. Arce, "Wavelet transfrom based watermark for digital images," *Optics Express* **3**(12), 497 (1998).
16. J. R. Kim and Y. S. Moon, "A robust wavelet-based digital watermark using level-adaptive thresholding," in *Proc. IEEE Int. Conf. Image Processing (ICIP)* (Kobe, Japan, Oct. 1999), p. 226.
17. T. D. Hien, Z. Nakao, and Y. W. Chen, "RDWT/ICA for image authentication," in *Proc. Fifth IEEE International Symposium on Signal Processing and Information Technology* (Dec. 2005), p. 805.
18. M. Barni, F. Bartolini, and A. Piva, "Improved wavelet-based watermarking through pixel-wise masking," *IEEE Trans. Image Processing* **10**(5), 783 (2001).
19. A. S. Lewis and G. Knowles, "Image compression using the 2-D wavelet transform," *IEEE Trans. Image Processing* **1**(2), 244 (1992).
20. J. M. Shapiro, "Embedded image coding using zerotrees of wavelet coefficients," *IEEE Trans. Signal Processing* **41**(12), 3445 (1993).
21. M. S. Hsieh, D. C. Tseng and Y. H. Huang, "Hiding digital watermarks using multiresolution wavelet transform," *IEEE Trans. Ind. Electron.* **48**(5), 875 (2001).
22. S.-H. Wang, Y.-P. Lin, "Wavelet tree quantization for copyright pretection water-

marking," *IEEE Trans. Image Processing* **13**(2), 154 (2004).
23. X.-D. Zhang, J. Feng, and K.-T. Lo, "Image watermarking using tree-based spatial-frequency feature of wavelet transform," *Journal of Visual Comm. and Image Representation* **14**(4), 474 (2003).
24. Y. Lao and Y. F. Zheng, "A tree-structure based logo watermarking scheme," in *Proc. the Sixth World Congress Intelligent Control and Automation* (Dalian, China, June 2006), p. 10365.
25. L. Xie and G. R. Arce, "Joint wavelet compression and authentication watermarking," in *Proc. IEEE Int. Conf. Image Processing (ICIP)* (Chicago, IL, USA, Oct. 1998), p. 427.
26. G. Wu and E. -H Yang, "Joint watermarking and compression using scalar quantization for maximizing robustness in the presence of additive Gaussian attacks," *IEEE Trans. Signal Processing* **53**(2), 834 (2005).
27. C. T. Hsu and J. L.Wu, "Multiresolution watermarking for digital images," *IEEE Trans. Circuits and Systems II: Analog and Digital Signal Proc.* **45**(8), 1097 (1998).
28. X. Niu, S. Sun and W. Xiang, "Multiresolution watermarking for video based on gray-level digital watermark," *IEEE Trans. Consumer Electron.* **46**(2), 375 (2000).
29. D. Kundur and D. Hatzinakos, "Toward robust logo watermarking using multiresolution image fusion principles," *IEEE Trans. Multimedia* **6**(1), 185 (2004).
30. A. A. Reddy and B. N. Chatterji, "A new wavelet based logo-watermarking scheme," *Pattern Recognition Lett.* **26**, 1019 (2005).
31. G. Xie and H. Shen, "A new fusion based blind logo-watermarking algorithm," *IEICE Trans. on Information and Systems* **E89-D**, 1173 (2006).
32. G. Xie and H. Shen, "Blind grayscale logo watermarking based on image fusion principles," *Abstracts. IEEE-Eurasip Nonlinear Signal and Image Processing* (2005), p. 5.
33. E. First and X. Qi, "A composite approach for blind grayscale logo watermarking," in *Proc. IEEE Int. Conf. Image Processing (ICIP)* (San Antonio, TX, USA, Sept. 2007), p. 265.
34. Y. Lao and Y. F. Zheng, "Optimal rate allocation for logo watermarking," in *Proc. IEEE Int. Conf. Image Processing (ICIP)* (San Antonio, TX, USA, Sep. 2007), p. 269.
35. D. S. Taubman and M. W. Marcellin, *JPEG2000: Image Compression Fundamentals, Standards and Practice*, (Kluwer Academic Publishers, 2002).
36. I. Daubechies, "Recent results in wavelet applications," in *Wavelet Applications V, H. Szu (ed.), Proc. SPIE* **3391**, 29 (1998).

Photo and Bibliography

Yuanwei Lao received the B.S. and M.S. degrees from the Department of Information Science and Electronics Engineering at Zhejiang University, Hangzhou, China, in 2000 and 2003, respectively. He is currently working toward the Ph.D. degree in the Department of Electrical and Computer Engineering at The Ohio State University, Columbus, Ohio. His research interests include image/video processing, pattern recognition and their multimedia applications.

Yuan F. Zheng (F'97) received the B.S. degree from Tsinghua University, Beijing, China, in 1970 and the M.S. and Ph.D. degrees in electrical engineering from The Ohio State University (OSU), Columbus, in 1980 and 1984, respectively.

From 1984 to 1989, he was with the Department of Electrical and Computer Engineering at Clemson University, Clemson, SC. Currently, he is Professor and was the Chairman of the Department of Electrical and Computer Engineering from 1993 to 2004 at The OSU, where he has been since 1989. From 2004 to 2005, he spent a sabbatical year at the Shanghai Jiao Tong University, Shanghai, China, where he continues to be involved as Dean of the School of Electronic, Information and Electrical Engineering for part-time administrative and research activities. His research interests include image and video processing for compression, object classification, object tracking, and robotics for which his current activities are in robotics and automation for high-throughput applications in biology studies. His research has been supported by the National Science Foundation, Air Force Research Laboratory, Office of Naval Research, Department of Energy, DAGSI, and ITEC-Ohio. He was and is on the Editorial Board of five international journals.

Dr. Zheng received the Presidential Young Investigator Award from Ronald Reagan in 1986, and the Research Awards from the College of Engineering of The OSU in 1993, 1997, and 2007, respectively. He and his students received the Best Student Paper or Best Conference Paper Awards several times, and received the Fred Diamond Award for Best Technical Paper from the Air Force Research Laboratory in 2006.